Nanocomposite Structure Based on Silylated MCM-48 and Poly(vinyl acetate)

Jing He,* Yanbin Shen, Jia Yang, David G. Evans, and Xue Duan*

Education Ministry Key Laboratory of Science and Technology of Controllable Chemical Reactions, Beijing University of Chemical Technology, Beijing 100029, P. R. China

Received September 24, 2002. Revised Manuscript Received April 11, 2003

As-synthesized MCM-48 was modified via silylation with $Cl-Si(CH_3)_3$. The resulting silylated MCM-48 possesses a well-ordered long-range structure, a narrow distribution of nanosized pore diameters, a high mesoporous volume, a large specific surface area, and, most significantly, a hydrophobic surface. A nanocomposite structure based on silylated MCM-48 and poly(vinyl acetate) (PVAc) has been prepared through both in situ polymerization and incorporation of preformed polymer. Characterization by FT-IR, XRD, and N_2 adsorption−desorption techniques indicates the latter method is more effective than the in situ polymerization method. The composites obtained by addition of the PVAc/silylated MCM-48 particles to a PVAc matrix have significantly enhanced mechanical performance, including toughness and elasticity, when compared with PVAc itself or with composites derived from PVAc and pure silylated MCM-48 or precipitated silica.

Introduction

Incorporation of nanosized inorganic particles in a polymer matrix has been the subject of much recent research[1−3] because the resulting nanocomposites have significantly better mechanical properties than the polymer itself. Polymers can be reinforced by particles such as precipitated silica,[4−9] titania,[7] and silica−titania oxides.[10] They can also be reinforced by a phase with only two dimensions on the nanometer scale such as cellulose whiskers.[11] Natural or synthetic clays such as layered silicates and layered double hydroxides are another possible reinforcing phase that, having the shape of platelets, have only one nano-level dimension.[12−21] Different ways of increasing the dispersion of the inorganic additives in the resulting nanocomposite materials have been widely investigated. Several sol−gel techniques[1] have been developed for the preparation of particle-reinforced nanocomposites, including dissolving preformed polymer in sol−gel precusor solutions,[22,23] simultaneous formation of organic and inorganic phases through the synchronous polymerization of the organic monomer and the sol−gel precursors,[22] and in situ precipitation of inorganic particles in the polymer phase.[6,7] For clay-reinforced nanocomposites, the available preparation techniques include in situ polymerization of intercalated monomers,[17] direct intercalation of extended polymer chains,[14,17,19,21] restacking of the exfoliated layers,[13,15,17] and in situ formation of inorganic layers in an aqueous polymer gel.[16] The development of inorganic additives that exhibit good interphase compatibility with a polymer matrix is also an important goal because the interphase interaction is paramount in determining the overall properties of the final composite materials.[8,9,15,19,22] Inorganic particles or clay layers, therefore, are often modified by surfactant-like materials or coupling agents to enhance their compatibility with the polymer. Zeolites are crystalline and porous aluminosilicates whose framework consists of well-defined pores and channels with pore openings between 0.3 and 1 nm. These pores and channels can be used as hosts for occluded polymer and are expected to provide extensive control over the structure of the

* Authors to whom correspondence should be addressed. E-mail: jinghe@263.net.cn or duanx@mail.buct.edu.cn.

(1) Wen, J.; Wilkes, G. L. *Chem. Mater.* **1996**, *8*, 1667.
(2) Hasegawa, N.; Kawasumi, M.; Kato, M.; Usuki, A.; Okada, A. *J. Appl. Polym. Sci.* **1998**, *67*, 87.
(3) Krishnamoorti, R.; Vaia, R. A.; Giannelis, E. P. *Chem. Mater.* **1996**, *8*, 1728.
(4) Motomatsu, M.; Takahashi, T.; Nie, H. Y.; Mizutani, W. H.; Tokumoto, H. *Polymer* **1997**, *38*, 177.
(5) Bokobza, L.; Garnaud, G.; Mark, J. E. *Chem. Mater.* **2002**, *14*, 162.
(6) Breiner, J. M.; Mark, J. E.; Beauage, G. *J. Polym. Sci., Part B: Polym. Phys.* **1999**, *37*, 1421.
(7) McCarthy, D. W.; Mark, J. E.; Clarson, S. J.; Schaefer, D. W. *J. Polym. Sci., Part B: Polym. Phys.* **1998**, *36*, 1191.
(8) Rajan, G. S.; Mark, J. E.; Seabolt, E. E.; Ford, W. T. *J. Macromol. Sci., Pure Appl. Chem.* **2002**, *A39*, 39.
(9) Premachandra, J.; Kumudinie, C.; Zhao, W.; Mark, J. E. *J. Sol−Gel Sci. Technol.* **1996**, *7*, 173.
(10) Wen, J.; Mark, J. E. *Rubber Chem. Technol.* **1994**, *67*, 806.
(11) Helbert, W.; Cavaill, J. Y.; Dufresne, A. *Polym. Comput.* **1996**, *17*, 604.
(12) Okada, A.; Kawasumi, M.; Usuki, A.; Kojima, Y.; Kurauchi, T.; Kamigaito, O. *Mater. Res. Soc. Proc.* **1990**, *171*, 45.
(13) Zhou, W.; Mark, J. E.; Unroe, M. R.; Arnold, F. E. *J. Macromol. Sci., Pure Appl. Chem.* **2001**, *A38*, 1.
(14) Strawhecker, K. E.; Manias, E. *Chem. Mater.* **2000**, *12*, 2943.
(15) Sur, G. S.; Sun, H. L.; Lyu, S. G.; Mark, J. E. *Polymer* **2001**, *42*, 9783.
(16) Carrado, K. A.; Xu, L. *Chem. Mater.* **1998**, *10*, 1440.
(17) Leroux, F.; Besse, J. P. *Chem. Mater.* **2001**, *13*, 3507.
(18) Alexandre, M.; Dubois, P. *Mater. Sci. Eng.* **2000**, *28*, 1.
(19) Vu, Y. T.; Mark, J. E.; Pham, L. H.; Engelhardt, M. *J. Appl. Polym. Sci.* **2001**, *82*, 1391.
(20) Carrado, K. A. *Appl. Clay Sci.* **2000**, *17*, 1.
(21) Wang, K. H.; Choi, M. H.; Koo, C. M.; Xu, M.; Chung, I. J.; Jang, M. C.; Choi, S. W.; Song, H. H. *J. Polym. Sci., Part B: Polym. Phys.* **2002**, *40*, 1454.
(22) Novak, B. M. *Adv. Mater.* **1993**, *5*, 422.
(23) Tong, X.; Tang, T.; Zhang, Q.; Feng, Z.; Huang, B. *J. Appl. Polym. Sci.* **2002**, *83*, 446.

10.1021/cm020938m CCC: $25.00
Published on Web 08/27/2003

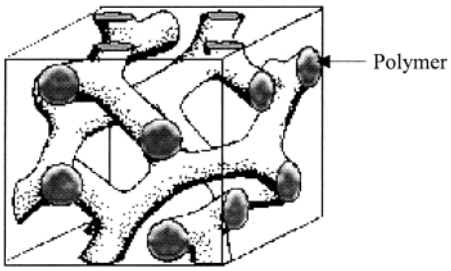

Figure 1. Schematic model of the nanocomposite structure based on MCM-48.

occluded polymer and over the associated host−guest interactions.[24−26] They could also allow optimization of the efficiency of elastomer reinforcement if some of the polymer chains could be encouraged to thread through the pores and channels. Zeolites have been used as additives in polymer fibers in such a way[27] in the hope that this molecular threading will provide an intimate interaction between the polymer chains and their inorganic host environment leading to novel reinforcement effects. Investigation of the reinforcing effects indicated that a zeolite having 1-nm cavities gave better reinforcement than one with 0.4 nm cavities, and the toughness was also improved for the larger-cavity zeolite. The discovery of the M41s family by Mobil researchers in 1992[28] opened up the possibility of occluding polymers in well-defined pores exceeding the diameter of those found in microporous zeolites. The tailorable nanosized pores and nano-thickness pore walls of mesoporous M41S materials, including MCM-41, MCM-48, and MCM-50, provide new opportunities for the construction of nanosized architecture. It can be expected that a polymer can either be introduced directly or produced through in situ polymerization of organic monomers inside the mesopores to form a nanocomposite structure based on MCM-41 or MCM-48. Because the organic phase extends along the channels to the openings in the nanocomposite structure, as shown in Figure 1, there should be a strong interaction between the nanocomposite and a continuous continuous polymer matrix, giving rise to well-dispersed particles. In our previous work[29] a nanocomposite structure based on MCM-41 and polyethylene formed through in situ polymerization of ethylene was prepared. This paper reports a nanocomposite structure based on MCM-48 and poly(vinyl acetate) (PVAc). Because MCM-48 has a three-dimensional arrangement of pores, rather than the one-dimensional arrangement in MCM-41, the interaction between the nanocomposite and a continuous polymer matrix in the final composites should be enhanced significantly.

Some attempts have been made to produce nanocomposites by threading or forcing polymer chains through the channels of mesoporous silica.[30,31] One goal is to determine the effects of constraining the geometry on the properties of the chains. Another goal is to investigate the possibility of in situ polymerization of MMA monomers inside the pores of mesoporous hosts to give molecular polymer composites. The focus of our work is on the formation of a nanocomposite structure in which the organic phase in the nanosized pores is isolated by the inorganic pore walls of MCM-48, and the effect of the nanocomposite structured particles as an additive or filler on the mechanical properties or performance of the final bulk composite materials.

Experimental Section

MCM-48 was synthesized under hydrothermal conditions using TEOS as Si source and cetyltrimethylammonium bromide (CTABr) as template. TEOS was first prehydrolyzed with NaOH solution and then added dropwise to the 25 wt % aqueous solution of CTABr. The final gel composition was SiO_2/Na_2O/CTABr/H_2O 1:0.21:0.65:62. The mixture was heated at 373 K for 7 days, and then filtered and dried at 373 K overnight to give the as-synthesized MCM-48 samples.

The modification of as-synthesized MCM-48 was carried out by silylation with $(CH_3)_3SiCl$. The mixture of as-synthesized MCM-48 and $(CH_3)_3SiCl$ was refluxed at 313−318 K for 36 h, followed by the addition of pyridine and refluxing for a further 18 h to give the silylated MCM-48. To prepare PVAc/silylated MCM-48 nanocomposite, PVAc was introduced by reaction of the inorganic host with a solution of vinyl acetate monomer or PVAc polymer in ethanol. The former is denoted the in situ polymerization method, and the latter is denoted the post-polymerization method. In the in situ polymerization method, silylated MCM-48 (0.25 g) was mixed with a solution of vinyl acetate (20 g) and benzoyl peroxide (0.1 g) in absolute ethanol (4 mL), followed by heating at 65 °C for 3 h in an inert atmosphere. In the post-polymerization method, a solution of vinyl acetate (20 g) and benzoyl peroxide (0.1 g) in absolute ethanol (4 mL) was first heated at 65 °C for 3 h in an inert atmosphere. Silylated MCM-48 (0.25 g) was then added and the mixture was shaken for 0.5 h.

The composite based on PVAc/silylated MCM-48 nanocomposite and a continuous PVAc matrix was prepared as follows. A known weight of PVAc was dissolved in acetone to produce a viscous fluid. A predetermined weight of nanocomposite (silylated MCM-48 with PVAc inside the pores) particles was then added to the stirred mixture to give a well-dispersed suspension. The suspensions were transferred to glass cells and left at ambient temperature until the residual solvent completely evaporated.

Pure silylated MCM-48 (without polymer chains introduced into the pores) and precipitated silica particles that had been modified following the same procedure as that for the silylation of MCM-48, were dispersed in a bulk PVAc matrix following the procedure described above, to produce control composites for comparison.

Powder XRD patterns were obtained using a Rigaku XRD-6000 instrument with Cu Kα source, step size of 0.02°, and 4 s per scan. The low-temperature N_2 adsorption−desorption experiments were carried out using a Quantachrome Autosorb-1 system. The pore size was calculated using the BJH method based on the N_2 desorption isotherm, and the specific surface area was calculated using the BET method based on the N_2 adsorption isotherm. The adsorption−desorption experiments of water and isopropanol vapors were performed on the same system. The FT-IR spectra were recorded on a Bruker Vector 22 spectrometer (resolution 4 cm^{-1}) at ambient temperature, with the samples being pressed into disks with

(24) Frisch, F. L.; Mark J. E. *Chem. Mater.* **1996**, *8*, 1735.
(25) Frisch, H. L.; Marref, S.; Xue, Y.; Beaucage, G.; Pu, Z.; Mark, J. E. *J. Polym. Sci., Part A: Polym. Chem.* **1996**, *34*, 673.
(26) Moller, K.; Bein, T.; Fischer, R. X. *Chem. Mater.* **1998**, *10*, 1841.
(27) Pu, Z.; Mark, J. E.; Beaucage, G. *Rubber Chem. Technol.* **1999**, *72*, 138.
(28) Beck, J. S.; Vartuli, C.; Roth, W. J.; Leonowicz, M. E.; Kresge, C. T.; Achmitt, K. D.; Chu, C. T.-W.; Olson, D. H.; Sheppard, E. W.; McCullen, S. B.; Higgins, J. B.; Schlenker, J. L. *J. Am. Chem. Soc.* **1992**, *114*, 10834.
(29) He, J.; Evans, D. G.; Duan, X.; Howe, R. F. *J. Porous Mater.* **2002**, *9*, 49.
(30) Moller, K.; Bein, T.; Fischer, R. X. In *Proceedings of the 12th International Zeolite Conference*; Treacy, M. M. J., Ed.; Materials Research Society: Warrendale, PA, 1999; p 2209.
(31) Moller, K.; Bein, T.; Fischer, R. X. *Chem. Mater.* **1999**, *11*, 665.

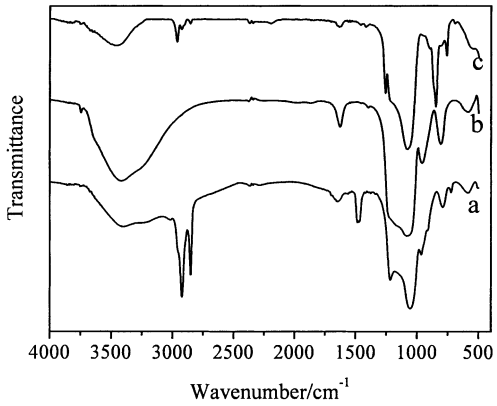

Figure 2. FT-IR spectra of (a) as-synthesized, (b) calcined, and (c) silylated MCM-48.

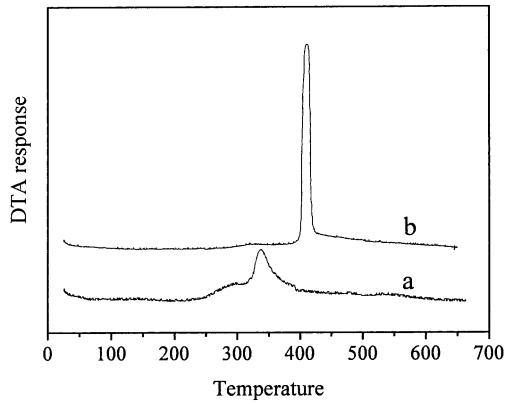

Figure 3. DTA curves of (a) as-synthesized and (b) silylated MCM-48.

KBr. TEM micrographs were taken on a Jeol J1M-2010 transmission electron microscope. The elemental analysis was carried out on a Carlo Erba 1106 elemental analysis system. The resolution limit was 0.3 wt %. The particle size distribution was measured using a Malvern Mastersizer 2000 laser particle size analyzer. The mechanical properties of the composites were measured on an Instron tester according to the standard method described in ASTM D638-81. The sample films were cut into long strips with approximate dimensions of 20 × 1.5 × 55 mm. Elongation measurements were conducted on the strips at ambient temperature under a humidity of 70%. The extension rate was 200 mm/min. Density measurements were carried out according to the standard method described in GB 217-81.

Results and Discussion

Modification of MCM-48 by Silylation. Figure 2 shows the FT-IR spectra of the as-synthesized MCM-48, its calcination product, and the material obtained by modification by silylation with $(CH_3)_3SiCl$. Comparing the silylated MCM-48 with the as-synthesized sample, the intensities of the bands at 2920 cm^{-1} and 2855 cm^{-1} characteristic of stretching vibrations of $-(CH_2)_n-$ groups decrease markedly, and the bands at 1480 cm^{-1} and 1223 cm^{-1} characteristic of bending vibrations of $-(CH_2)_n-$ disappear. Bands at 2960 cm^{-1} characteristic of $-CH_3$, at 1258 cm^{-1} characteristic of $-Si(CH_3)_3$, and at 852 cm^{-1} and 764 cm^{-1} characteristic of Si−C stretching vibrations appear, which are absent in the spectra of the as-synthesized and calcined MCM-48. These results indicate that the organic template used in the synthesis has been removed in the modification process and that the $-Si(CH_3)_3$ groups have been grafted onto the surface of MCM-48.

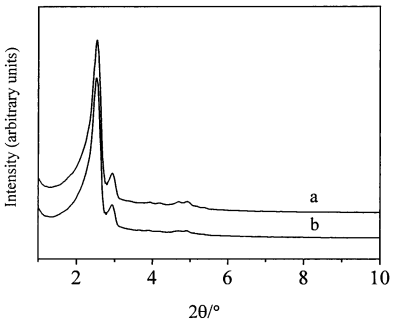

Figure 4. XRD patterns of (a) as-synthesized and (b) silylated MCM-48.

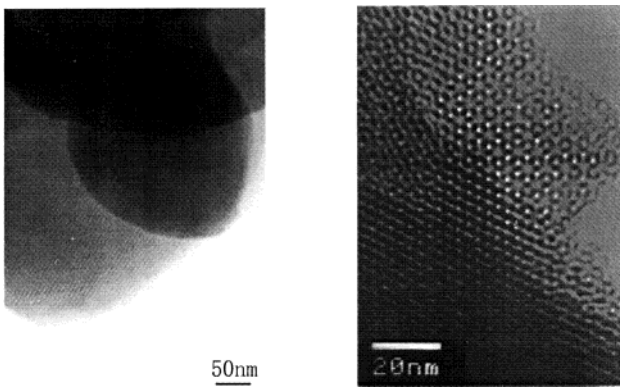

Figure 5. TEM micrograph of silylated MCM-48.

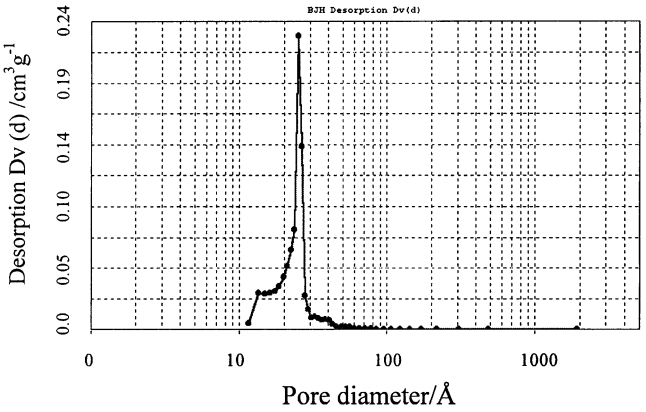

Figure 6. Pore size distribution of silylated MCM-48.

Figure 3 shows the DTA curves of the as-synthesized and silylated MCM-48. For the as-synthesized MCM-48, the DTA curve shows a broad exothermic peak with a shoulder at low temperature, which arises from decomposition of the organic template. The DTA curve for the silylated MCM-48, however, exhibits a single sharp exothermic peak, quite different from that of the as-synthesized MCM-48. The DTA curves confirm that the organic template has been completely removed by modification and the $-Si(CH_3)_3$ groups have been grafted onto the surface of MCM-48. The elemental analysis results indicate that no nitrogen is present in the silylated MCM-48, whereas the nitrogen content of the as-synthesized MCM-48 is 1.99 wt %. The analytical data are therefore consistent with the FT-IR and DTA results.

Figure 4 shows the XRD patterns of the as-synthesized and silylated MCM-48. The characteristic reflec-

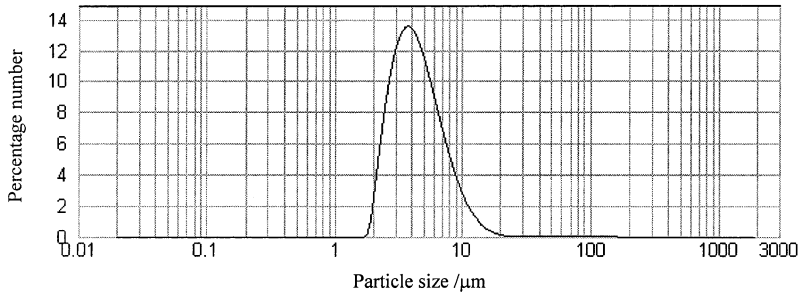

Figure 7. Particle size distribution of silylated MCM-48.

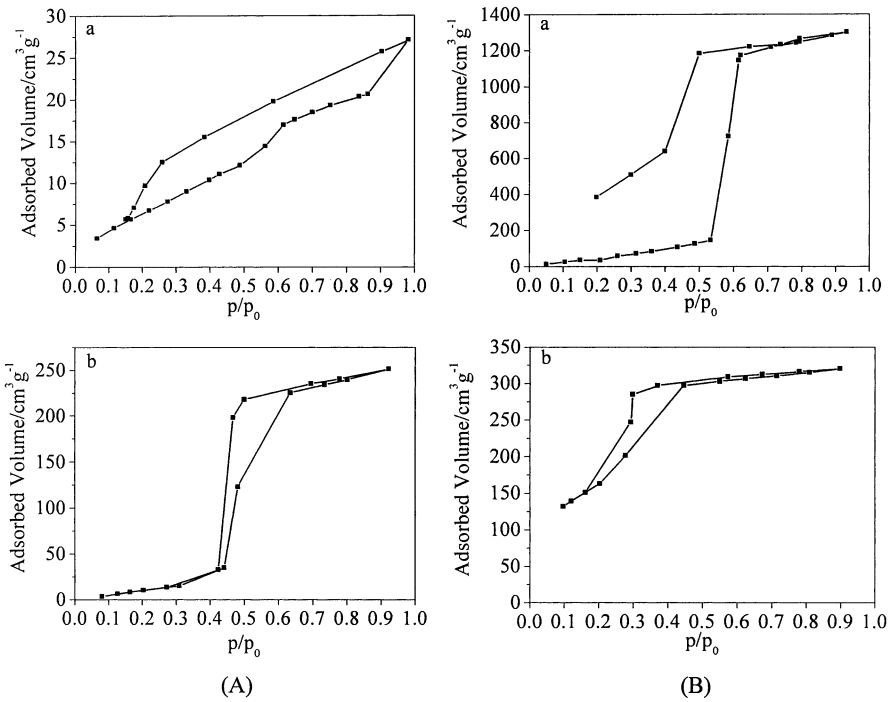

Figure 8. Adsorption−desorption isotherms of (a) water and (b) 2-propanol vapors for (A) silylated MCM-48 and (B) calcined MCM-48.

tions of a well-ordered cubic structure are present in both cases[5] indicating that silylation has no adverse effects on the long-range structure. The well-ordered array of channels can be clearly observed by TEM as shown in Figure 5. The pore size distribution shown in Figure 6 indicates that the silylated MCM-48 possesses a narrow distribution of nanosized pores with a modal pore diameter of 2.5 nm. The material has a specific surface area of 1172 m^2/g and a mesopore volume of 0.75 cm^3/g. This suggests that silylation has no adverse effects on the ordered mesoporous structure of MCM-48, consistent with the XRD results. The silylated MCM-48 possesses the structure and properties required of the inorganic component of the above-mentioned type of nanocomposite structure.

The particle size distribution for the silylated MCM-48 ranges from 1 to 10 μm with a single modal value based on number distribution, as shown in Figure 7. The maximum in the distribution is located at approximately 4 μm. The d (0.5) and d (0.9) values are 4.2 μm and 8.2 μm, respectively.

The surface hydrophobicity/hydrophilicity of silylated MCM-48 was evaluated by water and isopropanol vapor adsorption experiments. For comparison, the surface properties of calcined MCM-48 were also investigated. The water and isopropanol vapor adsorption−desorption isotherms of both calcined and silylated MCM-48 are typical of type IV as shown in Figure 8. The water vapor adsorption−desorption isotherms of the silylated MCM-48 exhibit a closed hysteresis loop characteristic of a hydrophobic surface, in contrast to the open hysteresis loop characteristic of a hydrophilic surface observed for the calcined MCM-48. The isotherms in terms of liquid volume of water and isopropanol, shown in Figure 9, indicate that the silylated MCM-48 has much a higher adsorption capacity for isopropanol than for water, and also exhibits a much lower adsorption capacity for water than the calcined MCM-48. The pore volumes calculated from N_2, water, and isopropanol adsorption are listed in Table 1. For silylated MCM-48, the total pore volume from N_2 or isopropanol adsorption is much higher than that from water adsorption. The total pore volume from water adsorption for silylated MCM-48 is also much lower than that for calcined MCM-48, although the total pore volumes from N_2 or isopropanol adsorption for the former are only slightly less than those of the latter. The results from the water and isopropanol vapor adsorption experiments indicate that the surface of silylated MCM-48 shows a much lower affinity to water molecules, suggesting that the silylation with $-Si(CH_3)_3$

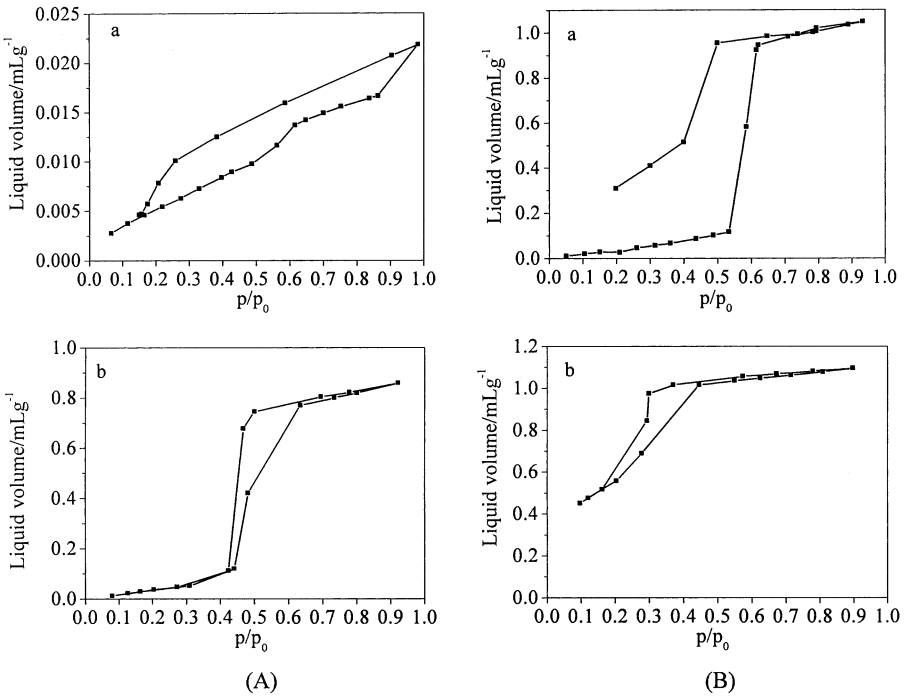

Figure 9. Adsorption−desorption isotherms as liquid volume of (a) water and (b) 2-propanol for (A) silylated MCM-48 and (B) calcined MCM-48.

Table 1. Total Pore Volumes (approximate $p/p_o \leq 0.90$) Calculated from N_2, Isopropanol, and Water Adsorption for Silylated and Calcined MCM-48

	N2 adsorption	2-propanol adsorption	water adsorption
silylated MCM-48	0.85	0.86	0.017
calcined MCM-48	1.17	1.09	1.04

significantly increases the hydrophobicity of the MCM-48 surface, which is expected to favor the introduction of polymer into the interior.

Combination of PVAc with MCM-48. *Introduction of PVAc by the in situ Polymerization Method.* The FT-IR spectrum of the nanocomposite with silylated MCM-48 prepared by the in situ polymerization method is shown in Figure 10. The presence of bands characteristic of $-(CH_2)_n$, groups at 2930 cm^{-1} and 2860 cm^{-1}, C−O groups in −COOC− moieties at 1240 cm^{-1}, C═O groups in −COOC− moieties at 1724 cm^{-1}, and $-CH_3$ groups at 1380 cm^{-1}, which are all absent in the spectrum of the silylated MCM-48 precursor, indicates that a PVAc organic phase has been produced and integrated with the silylated inorganic MCM-48 host.

The XRD pattern for the nanocomposite prepared by the in situ polymerization method, shown in Figure 11, exhibits the reflections characteristic of a well-ordered cubic structure similar to silylated MCM-48 itself.

Figure 12 shows the N_2 adsorption−desorption isotherms for the nanocomposite prepared by the in situ polymerization method. For comparison, the isotherms for silylated MCM-48 are also shown. In contrast to the silylated MCM-48, the nanocomposite exhibits a much lower and much less steep increase at approximately $p/p_o = 0.30$. The mesoporous volume decreases from 0.75 cm^3/g for the silylated MCM-48 to 0.07 cm^3/g for the nanocomposite, and the specific surface area falls from 1172 m^2/g to 101 m^2/g. Because both the mesoporous volume and surface area decrease by 1 order of magnitude, this strongly suggests that most of mesopore volume has been occupied by PVAc formed in situ inside the channels of silylated MCM-48.

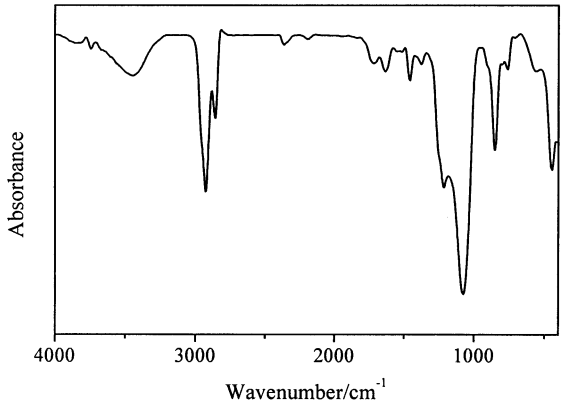

Figure 10. FT-IR spectrum of the nanocomposite prepared by the in situ polymerization method.

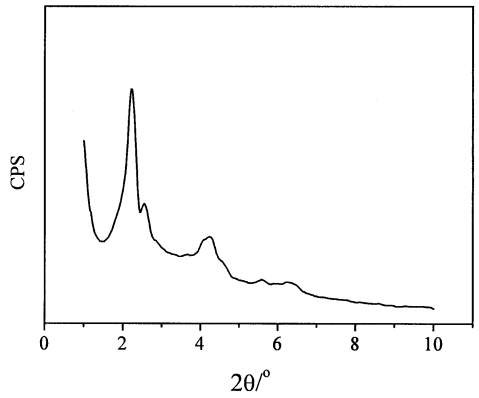

Figure 11. XRD pattern of the PVAc/silylated MCM-48 nanocomposite prepared by the in situ polymerization method.

Introduction of PVAc by the Post-Polymerization Method. Figure 13 shows the N_2 adsorption−desorption

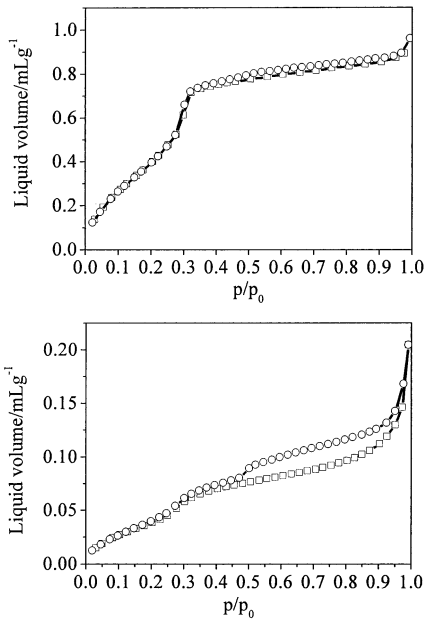

Figure 12. N_2 adsorption−desorption isotherms of (a) silylated MCM-48 and (b) PVAc/silylated MCM-48 nanocomposite prepared by the in situ polymerization method.

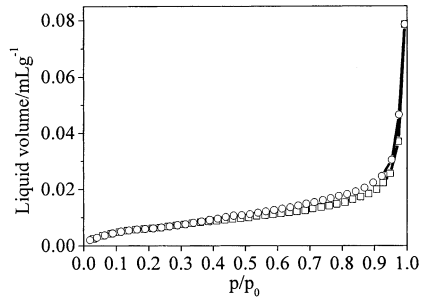

Figure 13. N_2 adsorption−desorption isotherms of the PVAc/silylated MCM-48 nanocomposite prepared by the post-polymerization method.

isotherms of the nanocomposite produced by incorporation of preformed PVAc polymer. In contrast to the silylated MCM-48 precursor, the PVAc/MCM-48 nanocomposite shows a type III adsorption isotherm typical of nonporous solids. The specific surface area decreased dramatically from 1172 m^2/g for silylated MCM-48 to 15 m^2/g for the PVAc/MCM-48 nanocomposite, and the mesoporous volume decreased from 0.75 cm^3/g to 0.009 cm^3/g. Both the surface area and mesoporous volume decreases by 2 orders of magnitude, suggesting complete occupancy of the mesopores by PVAc that has been introduced into the channels of MCM-48.

Figure 14 shows the XRD pattern of the nanocomposite prepared by the post-polymerization method. The XRD pattern exhibits the characteristic reflections of a well-ordered cubic structure similar to that of MCM-48 itself.

If the decrease in the N_2 adsorption volume is indeed caused by the penetration of polymer chains into the channels of silylated MCM-48, the data suggest that a nanocomposite structure based on silylated MCM-48 and PVAc can be formed by either in situ polymerization or post-polymerization methods. The possibility that the decrease in N_2 adsorption volume may be caused by the decrease in the accessibility of nitrogen to the interior surface of silylated MCM-48 cannot be definitely ex-

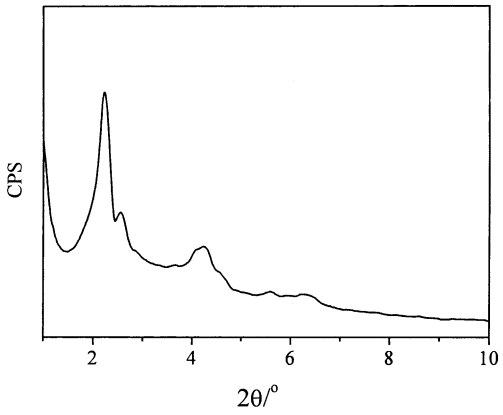

Figure 14. XRD pattern of the PVAc/silylated MCM-48 nanocomposite prepared by the post-polymerization method.

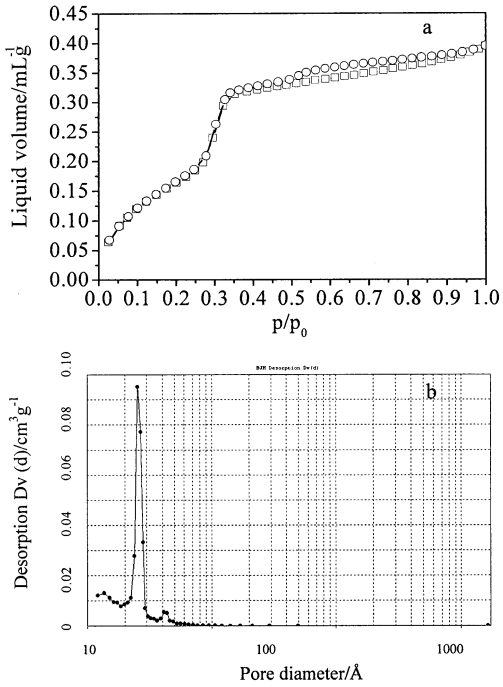

Figure 15. N_2 adsorption−desorption isotherms (a) and pore size distribution (b) of a control nanocomposite prepared through dispersion of silylated MCM-48 in PVAc.

cluded however. The density of the nanocomposite was therefore investigated. For silylated MCM-48 the density is 0.33 g/cm^3. For the nanocomposite formed by in situ polymerization or post-polymerization methods, the density increases to 1.08 g/cm^3 and 1.11 g/cm^3, respectively. The increase in the density is consistent with occupancy of the pores of silylated MCM-48 host by PVAc. The polymer chains have indeed penetrated into the channels, rather than being located only at the pore openings. Whereas the latter would also decrease the accessibility to nitrogen of the interior surface of MCM-48, it would not have a significant effect on the density. It can be concluded from the above results, therefore, that a well-ordered true nanocomposite structure has been produced.

A control composite prepared by dispersion of silylated MCM-48 in a PVAc polymer solution has been characterized by N_2 adsorption experiments for comparison, as shown in Figure 15. The N_2 adsorption−desorption isotherm is typical of type IV with a significant steep increase at $p/p_o \approx 0.30$. A narrow pore size

Figure 16. TEM micrograph of the PVAc/silylated MCM-48 nanocomposite prepared by the post-polymerization method.

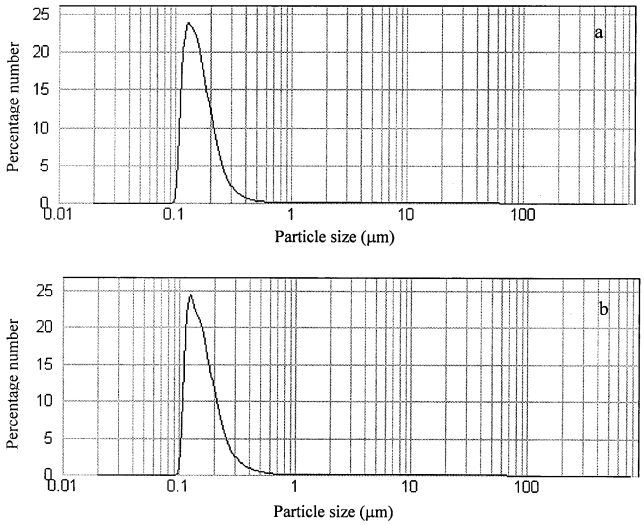

Figure 17. Particle size distribution of PVAc/silylated MCM-48 nanocomposite prepared by (a) in situ polymerization method and (b) post-polymerization method.

distribution is observed with a maximum of 2.5 nm in the distribution. The mesopore volume is 0.32 cm^3/g and the surface area is 440 m^2/g. The pore structure characteristics are similar to those of silylated MCM-48, except that the mesopore volume and surface area decrease due to the presence of PVAc in the sample. The mesopore volume and surface area are still high in comparison with those of the nanocomposites prepared using silylated MCM-48 with PVAc already in the channels, however. This suggests that there has been only partial penetration of polymer into the vacant channels of silylated MCM-48.

The TEM micrograph for the nanocomposite prepared by the post-polymerization method using silylated MCM-48 with PVAc already in the channels is shown in Figure 16. It shows the presence of the same pore structure as that of the precursor. It has previously been suggested[26] that a well-defined crystal surface indicates that polymer chains are mainly occluded inside the pores of the host. The TEM micrograph in Figure 16 suggests that the nanocomposite has well-ordered channels similar to those of silylated MCM-48 itself, consistent with the XRD results.

The particle size distribution curves for the nanocomposites prepared by in situ polymerization and post-polymerization methods are illustrated in Figure 17.

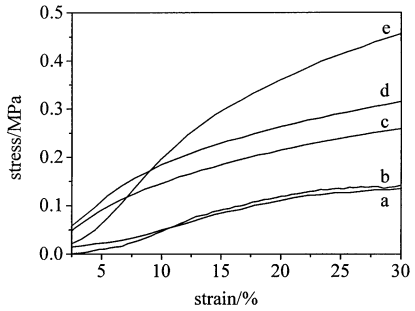

Figure 18. Stress−strain curves of PVAc-based composites with different additives: (a) PVAc matrix; (b) silylated MCM-48, 4%; (c) silylated silica particles, 4%; (d) PVAc/silylated MCM-48 nanocomposite, 4% of equivalent silylated MCM-48; (e) PVAc/silylated MCM-48 nanocomposite, 11% of equivalent silylated MCM-48.

Table 2. Tensile Properties of PVAc-Based Composites Using PVAc/Silylated MCM-48 Nanocomposites, Silylated MCM-48, and Silylated SiO_2 Particles as Additives

additives	content of additive (wt.%)	tensile modulus (MPa)	Ts (Mpa)	Eb (%)	toughness (MPa)
none	0	0.44	0.25	891	160
PVAc/silylated MCM-48 nanocomposite particles	7.41 [4.31][a]	0.67	0.59	719	372
	19.36 [11.26][a]	1.95	0.91	754	585
silylated MCM-48	4.31	0.63	0.30	509	126
modified silica particles	4.31	1.63	0.45	594	229

[a] Equivalent wt % of MCM-48.

This shows that the bulk form of the two nanocomposites is very similar. The maximum in the distribution is 0.13 μm and the value of d (0.5) is 0.15 μm in each case. The values of d (0.9) for the nanocomposites prepared by in situ polymerization and post-polymerization methods are 0.24 and 0.25 μm, respectively. This confirms that the large difference in N_2 adsorption properties discussed above (Figures 12 and 13) is indicative of a difference in the PVAc content inside the channels. The post-polymerization method is more effective than the in situ polymerization method in forming an intra-particle nanocomposite. Although the diffusion of the VAc monomer into the pores is presumably faster than that of PVAc, the steric constraints imposed by the channels may inhibit the in situ formation of PVAc chains.

Comparison of Figures 7 and 17 clearly demonstrates that introduction of polymer into silylated MCM-48 leads to a marked decrease in the particle size, from 4.0 μm to 0.1−0.2 μm. This suggests that the difficulty in dispersing inorganic particles to nano-dimensional size, which is common with conventional inorganic particles such as SiO_2, may be readily overcome in this case.

Composites Based on PVAc/silylated MCM-48 Nanocomposite Particles and PVAc Matrix. The PVAc/silylated MCM-48 nanocomposite was used as an additive with a PVAc matrix. Figure 18 shows the stress−strain curves of the resulting composites with different PVAc/silylated MCM-48 nanocomposite content. The mechanical performances of the resulting composites are summarized in Table 2. For comparison, the mechanical properties of composites based on pure silylated MCM-48 (without preintroduction of PVAc chains into the mesopores of silylated MCM-48 host) or

silylated precipitated SiO_2 particles and PVAc matrix are also shown in Figure 18 and Table 2. The particle size of the modified SiO_2 is similar to that of the silylated MCM-48 particles. The results show that the addition of PVAc/silylated MCM-48 nanocomposite particles significantly increases tensile strength (Ts), tensile modulus, and toughness, while it slightly decreases the elongation at break (Eb). The tensile modulus increases by 50∼340%, and both tensile strength and toughness increase by 100∼260%. The elongation at break decreases by less than 20%. The results indicate that the addition of PVAc/silylated MCM-48 nanocomposite particles significantly enhances the mechanical performance of the PVAc matrix. Increasing the content of nanocomposite particles increases the tensile modulus, toughness, and tensile strength, while exhibiting no significant effect on the elongation at break. The increase in tensile modulus expressing the stiffness of a material at the start of a tensile test and its tensile strength is mainly attributed to the inclusion of rigid content in the elastomeric matrix.[32] In the case of the control composite based on pure silylated MCM-48 and PVAc matrix however, the increase in tensile modulus and tensile strength is less significant, and the elongation at break is reduced more markedly, than for the material based on the preformed PVAc/silylated MCM-48 nanocomposite, when the content of silylated MCM-48 is similar. The pure silylated MCM-48 particles give a negligible improvement in the toughness of the resulting composites. The control composite based on silylated silica particles and a continuous PVAc matrix exhibits a much higher tensile modulus and lower tensile strength, elongation at break, and toughness than the composites based on the nanocomposite structured particles and PVAc polymer. The elongation at break for the composite based on the silica particles is similar to that for the composite based on pure silylated MCM-48. The main difference between the composites based on the silica particles and the nanocomposite structured particles is that the former enhances the stiffness of the resulting composites.

It has been frequently demonstrated[18] that tensile strength is strongly influenced by the nature of the interactions between the matrix and the filler. For a composite system where interfacial adhesion is poor, little or no tensile stress enhancement is observed. The elongation at break, which expresses the elasticity of a composite, is usually reduced by incorporation of any rigid inorganic content.[32] By virtue of the presence of polymer chains inside the mesopores of silylated MCM-48, the nanocomposite structured particles prepared in this work exhibit great advantages over simple silylated MCM-48 particles, as far as improving the mechanical performance of the resulting composites is concerned. The advantages of the nanocomposite structured particles over precipitated silica particles may result from both the presence of polymer chains inside the channels of MCM-48 host and the larger interfacial area. The surface area of silylated MCM-48 is around 1000 m^2/g, whereas that of SiO_2 is approximately 300 m^2/g. Both the larger interfacial area and good interfacial adhesion contribute to the improvement in the mechanical properties of the composites prepared with the nanocomposite structured particles relative to those prepared with silica.

So far, the most promising inorganic fillers for nanocomposite and/or composite materials are natural and synthetic clays and silica particles. The polymer matrixes that have been studied include PMA;[5] HPBO and SPBT polymers;[9] PDMS;[27] polysulfones;[15] PVP, HPMC, PACN, PDDA, PANI, and PAM;[20] and Nylon-6, PMMA, PP, and PS.[18] In the case of silica−polymer composites, Mark and co-workers have carried out detailed investigations of the effects of particle distribution, and especially interfacial interaction, on mechanical properties of composites. On the basis of a comparison between materials showing presence and absence of interfacial covalent bonding, it was concluded that fillers have no reinforcing effect unless there is good polymer−filler interaction. TPM-silica, which can give covalent bonds with a PMA matrix, increases the tensile modulus more significantly than CP-silica filler, which has only weak physical interaction with the PMA matrix.[5,8] In the case of physical interfacial interactions, the filler particles do essentially nothing to improve the tensile modulus and strength of the composites and merely contribute to the void content of the material.[8] Clays and organically-modified clays have also been widely studied. Clay layers can be conventionally dispersed in a polymer matrix in two ways. Well-ordered, stacked multilayers result from the intercalation of polymer chains within the host clay layers. At the other extreme, delaminated materials in which the host layers have lost their registry are randomly dispersed in a continuous polymer matrix. A novel method has been developed by Carrado et al. in which the inorganic layers are formed in situ in a polymer gel.[16] The resulting structure can be thought of as a semi-exfoliated system in which small clay crystallites, intercalated by polymer and stacked to a small degree, are well dispersed within a continuous polymer matrix. This method ameliorates problems with the two conventional dispersal methods mentioned above. However, its application is limited by the requirement for polymer water-solubility. For the composites based on PVAc/silylated MCM-48 and PVAc matrix prepared in this work, although the interfacial interactions between silylated MCM-48 and PVAc inside the mesopores as well as between the nanocomposite particles and the PVAc matrix are all noncovalent interactions, the mechanical properties are significantly increased. In addition, the method is suitable for both water-soluble and water-insoluble polymers. The potentially most interesting and significant factor is that the polymer used to produce the nanocomposite structure inside the channels of MCM-48 can be altered according to the requirements of the final composite. It can be either the same as, or different from, the continuous polymer matrix, thereby providing the feasibility of finely tailoring the properties of the resulting composite. The nanocomposite structure can be expected to exhibit more significant advantages if it is used in a continuous polymer matrix which is more brittle and difficult to strengthen than PVAc, which is a very ductile polymer.

(32) Wang, S.; Xu, P.; Mark, J. E. *Rubber Chem. Technol.* **1991**, *64*, 746.

Conclusions

A nanocomposite structure based on silylated MCM-48 and PVAc can be prepared through in situ polymerization or post-polymerization methods. The latter is more effective in the formation of an intra-particle nanocomposite structure than the former. When the PVAc/silylated MCM-48 nanocomposite particles are used as an additive with a bulk PVAc matrix, they lead to an enhancement of the mechanical performance of the polymer. These particles also show significant advantages in improving the mechanical properties of PVAc matrix over those of the pure silylated MCM-48 and SiO_2 particles.

Acknowledgment. We are grateful to the National Natural Science Foundation of China for financial support (No. 59973004).

CM020938M